



HAL
open science

Strategies for the Controlled Covalent Double Functionalization of Graphene Oxide

Isabella Anna Vacchi, Shi Guo, Jesus Raya, Alberto Bianco, Cecilia
Ménard-Moyon

► **To cite this version:**

Isabella Anna Vacchi, Shi Guo, Jesus Raya, Alberto Bianco, Cecilia Ménard-Moyon. Strategies for the Controlled Covalent Double Functionalization of Graphene Oxide. Chemistry - A European Journal, 2020, 10.1002/chem.201905785 . hal-02926641

HAL Id: hal-02926641

<https://hal.science/hal-02926641>

Submitted on 31 Aug 2020

HAL is a multi-disciplinary open access archive for the deposit and dissemination of scientific research documents, whether they are published or not. The documents may come from teaching and research institutions in France or abroad, or from public or private research centers.

L'archive ouverte pluridisciplinaire **HAL**, est destinée au dépôt et à la diffusion de documents scientifiques de niveau recherche, publiés ou non, émanant des établissements d'enseignement et de recherche français ou étrangers, des laboratoires publics ou privés.

Strategies for the Controlled Covalent Double Functionalization of Graphene Oxide

Isabella A. Vacchi,^[a] Shi Guo,^[a] Jésus Raya,^[b] Alberto Bianco,^{*,[a]} and Cécilia Ménard-Moyon^{*,[a]}

^[a] CNRS, Immunology, Immunopathology and Therapeutic Chemistry, UPR 3572, University of Strasbourg, ISIS, 67000 Strasbourg (France)

^[b] Membrane Biophysics and NMR, Institute of Chemistry, UMR 7177, University of Strasbourg, Strasbourg (France)

E-mail: c.menard@ibmc-cnrs.unistra.fr and a.bianco@ibmc-cnrs.unistra.fr

Abstract

Graphene oxide (GO) is a versatile platform with unique properties that have found broad applications in the biomedical field. Double functionalization is a key aspect to design multifunctional GO with combined imaging, targeting, and therapeutic properties. Compared to non-covalent functionalization, covalent strategies lead to GO conjugates with a higher stability in biological fluids. However, only a few double covalent functionalization approaches have been developed so far. The complexity of GO makes the derivatization of the oxygenated groups difficult to control. We investigated the combination of a nucleophilic epoxide ring opening with the derivatization of the hydroxyl groups *via* esterification or the Williamson reaction. The conditions were selective and mild, thus preserving the structure of GO. Our strategy of double functionalization holds a high potential for different applications where the derivatization of GO with different molecules is needed, especially in the biomedical field.

Keywords

Carbon materials; Esterification; Protecting groups; Surface chemistry; Williamson reaction

Introduction

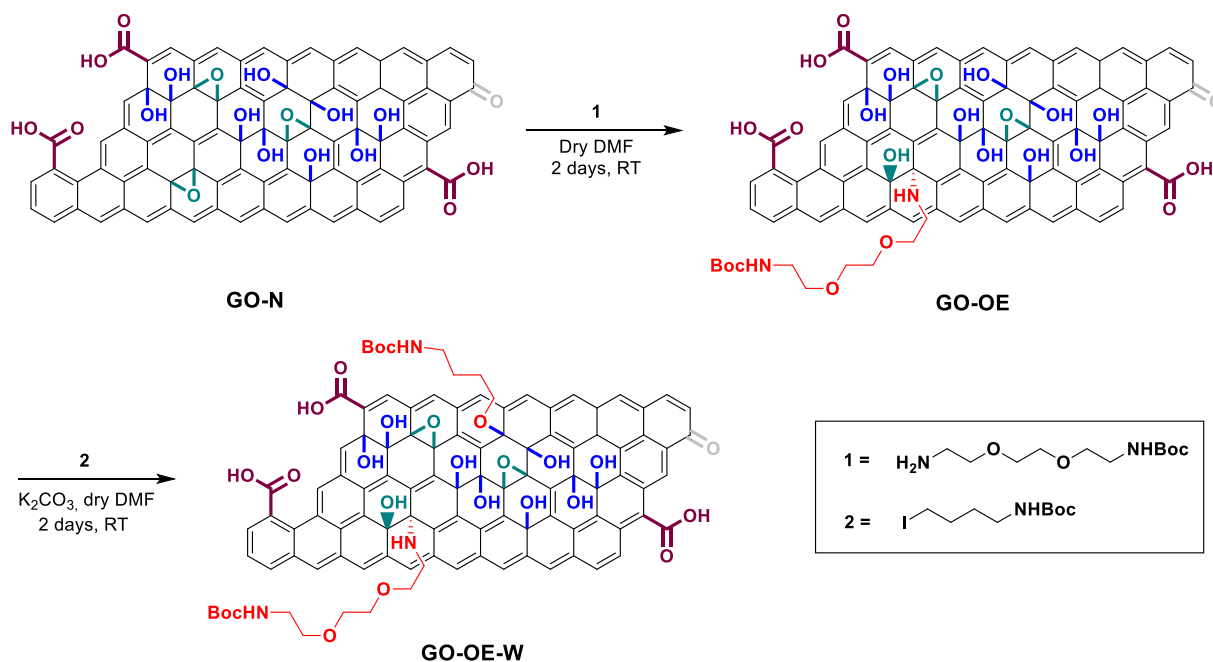
Graphene oxide (GO) has been extensively investigated in many fields,^[1,2] in particular in nanomedicine because of its excellent aqueous processability, amphiphilicity and the possibility of surface functionalization.^[3-5] In its reduced form it displays thermal and electrical conductivity that can be exploited for the development of biosensors.^[6,7] The large surface area and the chemical structure of GO enable several chemical modifications,^[8-10] making it an excellent platform for multifunctionalization through covalent and/or non-covalent approaches. Covalent functionalization is more stable compared to non-covalent interactions and this is preferable for biomedical applications as there is a risk of release of the bioactive molecules adsorbed onto the GO surface in the biological media.^[11] Multifunctionalization strategies allow to combine the properties of several molecules with those of GO. Until now, only few covalent double functionalization strategies of GO have been reported. Even if GO is composed of different functional groups, mainly epoxides, hydroxyls, and a little amount of carboxylic acids,^[12] most approaches mainly exploited the same functional groups on the surface of GO or different functional groups without any selectivity. Few research groups developed a double functionalization process targeting selectively two functional groups already present on the surface of GO such as the epoxides or hydroxyls, and the carboxylic acids.^[13-16] For instance, Imani *et al.* prepared multifunctionalized GO by derivatization of the hydroxyls using chloroacetic acid and sodium hydroxide, followed by amidation of the carboxylated GO with a mixture of polyethylene glycol diamine and octa-arginine.^[13] Rezaei *et al.* performed the Ugi reaction on carboxylated GO using cyclohexylisocyanide, an aldehyde and an amine derivative.^[14] In both studies the hydroxyls on the basal plane and the COOH groups at the edges of GO were exploited for functionalization. The combination of epoxide ring opening using an amine derivative followed by amidation of the carboxylic acids using a second amine-bearing compound has also been reported.^[15] In another approach Al-Jamal and coworkers synthesized GO doubly functionalized with an azide and an alkyne moiety.^[16] Sodium azide reacted as nucleophile to open the epoxides and the alkyne moiety was subsequently introduced by Steglich esterification of the carboxyl groups. However, GO had to be pre-treated with *m*-chloroperoxybenzoic acid before functionalization to increase the amount of epoxides on its surface. In addition, all these strategies involve a reaction exploiting the COOH groups at the edges of GO, and we previously demonstrated that they are present only in low amount,^[12] thus resulting in low levels of functionalization. Recently, we reported a simple and versatile strategy for the covalent double functionalization of GO based on the combination of epoxide opening by a thiol derivative and a Michael addition of the hydroxyls with benzoquinone.^[17] In this context, we wish to extend the possibilities of double functionalization of GO through selective derivatization of the epoxides and hydroxyls. For this purpose, we designed a strategy combining a

nucleophilic epoxide opening reaction with the derivatization of the hydroxyl groups by esterification or etherification (Williamson reaction). We used mild conditions (room temperature and mild base) to preserve the structure and properties of GO. Indeed, harsh conditions such as heating or the use of strong bases often cause partial reduction of GO, thus drastically decreasing its water dispersibility.^[18-21]

Results and Discussion

Combination of epoxide opening and Williamson reaction

The first double functionalization strategy we investigated was the combination of a nucleophilic epoxide opening and the Williamson reaction. We decided to perform first the opening of the epoxides by an amine derivative because the number of hydroxyl groups available for the subsequent Williamson reaction increases after the epoxide ring opening. The reaction was performed on GO from NanoInnova (named **GO-N**, see Materials and Methods part in Supporting Information). The Boc mono-protected triethylene glycol (TEG) diamine **1** was mixed to a suspension of GO in DMF obtaining **GO-OE** (OE stands for opening of epoxides) (Scheme 1).^[12] For the Williamson reaction **GO-OE** was mixed with the iodinated derivative **2** and K₂CO₃ in DMF leading to **GO-OE-W** (W stands for Williamson reaction).^[22] Potassium carbonate is commonly used to perform the Williamson reaction of phenol derivatives and it is mild enough to avoid reduction of GO.^[22] In addition, both reactions were performed at room temperature, thus preserving the structure of GO.



Scheme 1. Double functionalization approach combining the opening of the epoxides and the Williamson reaction (each reaction is shown only on one functional group for clarity reasons).

GO-N and **GO-OE-W** were characterized by transmission electron microscopy (TEM) (Figure S1a and b). The graphene sheets have a lateral dimension of a few micrometers and a wavy shape with folded edges. By comparison to **GO-N**, we found that the morphology of GO was preserved after the two-step derivatization.

We also characterized **GO-OE** and **GO-OE-W** by thermogravimetric analysis (TGA) under inert atmosphere (Figure S2). Because of thermal instability of GO due to labile oxygenated groups that makes the interpretation of the TGA data difficult,^[23-25] we also prepared control samples **GO-OE_CONT** and **GO-OE-W_CONT** by simply mixing **GO-N** in similar conditions but without adding **1** and **2** for the control reactions of the epoxide opening and the Williamson reaction, respectively (Scheme S1). Even though the conditions used for the reaction were mild, the control GO samples displayed a higher thermal stability due to some labile functionalities that were removed from the surface of GO.^[26-30] As a consequence, TGA is more useful in this case to compare the weight loss between samples of GO already functionalized. Nevertheless, the thermogravimetric curves of the functionalized samples, **GO-OE** and **GO-OE-W**, compared to their respective control samples did not show a significantly higher weight loss probably due to low molecular weight of the grafted molecules (Figure S2). However, **GO-OE-W** displayed a slightly higher weight loss above 300°C compared to **GO-OE**, which is indicative of successful Williamson reaction.

Characterization by X-ray photoelectron spectroscopy (XPS) allowed to determine the percentage of nitrogen introduced on **GO-N** (Figure S3). Values of 1.45% and 1.70% of nitrogen were found for **GO-OE** and **GO-OE-W**, respectively, while no nitrogen was found in **GO-N** (Table S1). There is a significant difference, even if not high, in the nitrogen percentage between the two steps of the double functionalization, indicating that both reactions happened. This result is supported by the XPS high resolution spectra confirming the introduction of the two functional chains. Indeed, in the O1s spectra of **GO-OE** the area percentage of the C=O peak that could be assigned to the urethane moiety of the Boc protecting group increases significantly (Figure S3). Unfortunately, the C1s peak does not bring insights on the outcome of the reaction due to the complexity of the deconvolution. In the N1s high resolution spectra of **GO-OE** and **GO-OE-W** a main peak centred at 399-400 eV was identified, which can be attributed to the amino and amide groups of **1** and **2** grafted onto GO.^[31] Thus, the XPS analysis confirmed the occurrence of both successive reactions. In addition, the C/O ratio did not change much (2.04 for **GO-N** vs. 2.30 and 2.38 for **GO-OE** and **GO-OE-W**, respectively), indicating that the conditions were mild enough to avoid reduction of GO. Finally, the level of functionalization was assessed using a colorimetric test (Kaiser test) that allows to determine the amount of primary amino groups present on GO. The amine loading was 145 and 175 µmol/g after treating **GO-OE** and **GO-OE-W** with a solution of HCl in 1,4-dioxane to cleave the Boc group (Scheme S2, Table S1).

We estimated that the level of functionalization was one amine every 347 and 287 carbon atoms, respectively (see Table S1 and part 3 in the SI for the explanations on the calculations). It is worth noting that the control samples **GO-OE_CONT** and **GO-OE-W_CONT** were also characterized by the Kaiser test after acidic treatment and no significant amine loading was found, which indicates that compounds **1** and **2** do not adsorb on the surface of GO. This result suggests that the functionalization is certainly covalent in the case of **GO-OE** and **GO-OE-W**. In addition, the control sample **GO-OE_CONT** revealed no trace of nitrogen by XPS, showing that there is no residual DMF in the sample. The level of functionalization was 145 $\mu\text{mol/g}$ of GO for the first step (epoxide opening), while the outcome for the Williamson reaction corresponds to the difference between the two loading values (30 $\mu\text{mol/g}$) (Table S1). Thus, the combination of these two reactions was successful. In our previous work the monofunctionalization of **GO-N** by the Williamson reaction gave an amine loading of 132 $\mu\text{mol/g}$.^[22] In comparison, the same reaction performed after the opening of the epoxides in the current study is not as efficient as expected. Different reasons could explain the difficulty to reach high loadings for the second reaction, for instance a steric hindrance due to the grafting of a high amount of compound **1** on GO and/or the loss of labile hydroxyl groups from the surface of GO during the different reaction steps.

To better investigate the second hypothesis related to the instability of the hydroxyl groups, we performed the double functionalization of GO by inverting the epoxide opening and the Williamson reaction. For this purpose, compound **2** was first added to **GO-N** in the presence of K_2CO_3 to get **GO-W** (Scheme S3). Then, compound **1** reacted with **GO-W** to open the epoxides giving **GO-W-OE**. The Kaiser test was performed after Boc deprotection (Table S1 and Scheme S2). The amine loading of **GO-W** and **GO-W-OE** was 106 and 145 $\mu\text{mol/g}$, respectively. We could deduce that the loading corresponding to the epoxide opening was only 39 $\mu\text{mol/g}$ in this case. Therefore, by inverting the order of both reactions a slightly lower loading was obtained for the first step (106 vs. 145 $\mu\text{mol/g}$ for epoxide opening), while the loading of the second step was increased by only 9 $\mu\text{mol/g}$. The functionalized GO samples were also characterized by XPS (Figure S4). For **GO-W** and **GO-W-OE** 0.96% and 1.57% of nitrogen were measured by XPS, respectively, while 0.6%N was found for the control sample **GO-W_CONT**, which is lower compared to **GO-W** (data not shown), indicating that there are probably traces of DMF in the sample. As before, similar changes were identified in the high resolution O1s and N1s spectra giving evidence of the introduction of amines protected by the Boc group. Furthermore, the C/O ratio was rather similar before and after functionalization (2.04 for **GO-N** vs. 2.39 and 2.08 for **GO-W** and **GO-W-OE**, respectively). The TGA curves of **GO-W** and **GO-W-OE** did not show significant differences in comparison with their

respective control samples **GO-W_CONT** and **GO-W-OE_CONT** prepared by simply mixing **GO-N** and **GO-W_CONT** in similar conditions but without compounds **2** and **1**, respectively (Figure S5 and Scheme S4). Again, the thermal instability of GO and the low molecular weight of the molecules grafted on GO makes the interpretation of the TGA data complicated. TEM showed that the morphology of the doubly functionalized GO was unaffected after both reactions (Figure S1c).

In this alternative approach the loading for the second reaction was only slightly increased compared to the first strategy. This suggests that, besides the instability of the hydroxyl groups, there must be another reason, such as steric hindrance, that hampers reaching a higher loading for the second step. Therefore, we decided to investigate further the first approach, which was the most efficient based on XPS and the Kaiser test, by optimizing the second step through the derivatization of the hydroxyl groups by esterification instead of the Williamson reaction because of potential higher reactivity.

Epoxide opening followed by esterification

We repeated the epoxide opening of **GO-N** by compound **1** giving again **GO-OE** (Scheme S5). The esterification of the hydroxyl groups with Boc-protected aminocaproic acid **3** was performed in the presence of 1-ethyl-3-(3-dimethylaminopropyl)carbodiimide (EDC) and 4-dimethylaminopyridine (DMAP) as coupling agents at room temperature to get **GO-OE-EST** (EST stands for esterification). As compounds **1** and **3** bear a primary amine protected with a Boc group, **GO-OE** and **GO-OE-EST** were treated in acid conditions to cleave the Boc moiety (Scheme S2 and S6). The amine loading obtained by the Kaiser test was 179 and 231 $\mu\text{mol/g}$ for **GO-OE** and **GO-OE-EST**, respectively, confirming the successful introduction of both molecules (Table S2). The epoxide opening led to a loading similar to the value obtained previously (145 $\mu\text{mol/g}$, Table S1). The level of functionalization for the esterification reaction was 52 $\mu\text{mol/g}$, which is higher compared to the Williamson reaction and the epoxide opening performed as second reaction (30 and 39 $\mu\text{mol/g}$, respectively). The level of functionalization for **GO-OE-EST** was estimated 1 amine every 218 carbon atoms, which is higher compared to **GO-OE-W** (1 every 287 C) (Table S1 and S2). Therefore, the hydroxyl groups are slightly more reactive towards esterification in comparison to the Williamson reaction. A control reaction was performed by treating **GO-N** in similar conditions of the epoxide opening but without the addition of compound **1** followed by mixing with compound **3** in the absence of the coupling agents giving **GO-OE_CONT** and **GO-OE-EST_CONT** (Scheme S7). The Kaiser test value obtained for **GO-OE-EST_CONT** after acidic treatment was negative (6 $\mu\text{mol/g}$) confirming the absence of **3** non-covalently adsorbed on GO.

XPS confirmed that both reactions occurred on the surface of **GO-N** as an introduction of 1.96 and 2.47% of nitrogen was detected for **GO-OE** and **GO-OE-EST**, respectively (Figure S6), whereas

only 0.44%N was found for the control sample **GO-OE_CONT** due to probable traces of residual DMF (data not shown). For this double functionalization strategy, the O1s spectra showed an increase of the C=O peak area due to the introduction of both **1** and **3**. The C/O ratio slightly increased from 2.04 for **GO-N** to 2.27 and 2.64 for **GO-OE** and **GO-OE-EST**, respectively, indicating that the structure of GO was not affected after functionalization. The N1s high resolution spectrum displayed the typical peak of the amine and amide at 399-400 eV, confirming the functionalization. We also performed carbon KLL Auger spectroscopy for all samples (Figure S6i). The analysis of these peaks gives an idea of the quantity of sp^2 and sp^3 carbon atoms present on GO.^[32,33] This estimation is obtained by calculating the distance between the maximum and the minimum binding energy of the first derivative of the C KLL spectra. There was no significant difference in distance among all the samples analyzed, demonstrating that the different reactions did not affect the structure of GO. We can notice that **GO-OE-EST** displayed closer maximum and minimum values, indicating a slightly more important content of sp^3 C atoms. This could be related to the sp^3 C atoms from the alkyl chains in compounds **1** and **3**.

TGA showed rather similar curves for both **GO-OE** and **GO-OE-EST** and their respective controls **GO-OE_CONT** and **GO-OE-EST_CONT**, giving no clear evidence of double functionalization of GO (Figure S7).

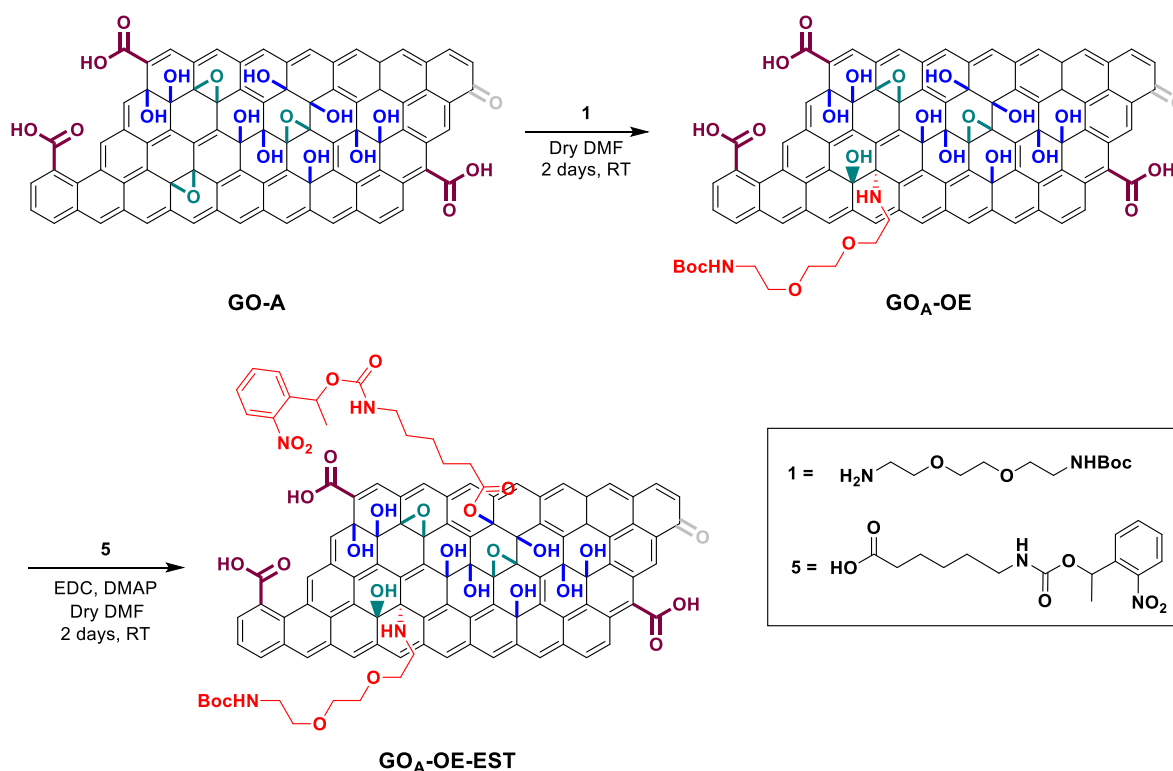
TEM confirmed the unchanged morphology of the doubly functionalized GO sheets (Figure S1d). Finally, **GO-OE-EST** was examined by quantitative ^{13}C direct polarization (DP) and cross polarization (CP) magic angle spinning (MAS) solid-state NMR (Figure S8). The peaks at ~ 60 and 70 ppm are attributed to the epoxides and hydroxyl groups, respectively, while the peak at ~130 ppm corresponds to the C=C bonds. We calculated the percentage of all peaks by integrating each peak after fitting (Table S3a). We estimated that **GO-N** contains 23% epoxides, 28% hydroxyls, and 37% C=C bonds. After the reactions, we noticed the appearance of peaks at 27 and 40 ppm that can be assigned to the Boc protecting group and the methylene moieties of compounds **1** and **3**, respectively. Moreover, the quantitative spectra showed a decrease in the intensity of the peak at ~60 ppm, confirming the opening of the epoxide ring (Figure S8, bottom spectrum). Unfortunately, we were not able to detect the peak of the ester function at ~170 ppm probably due to very low intensity.

Taken together, XPS, the Kaiser test, and MAS NMR confirmed the positive outcome of both reactions leading to doubly functionalized GO. Nevertheless, it should be taken into consideration that the loading of the second reaction was still much lower (52 $\mu\text{mol/g}$) compared to the esterification performed as mono-functionalization of **GO-N** (165 $\mu\text{mol/g}$ as published in our previous study).^[22] We think that reasonable explanations for such lower reactivity for the second functionalization reaction could be due to the combination of two phenomena: 1) the instability of some labile hydroxyl

groups on the surface of GO, and 2) localization confinement of the functional groups on islands that causes a steric hindrance for the second reaction because of the molecules introduced during the first step. Indeed, in the literature an island localization of the oxygenated functional groups on the surface of GO has been reported by many groups.^[34-37] Through aberration corrected TEM Erickson *et al.* observed that there are graphitic regions in GO up to 8 nm² and that the oxidized regions exhibit no order and have a minimal sp² bonding character.^[37] This type of structure was also confirmed by Zhou *et al.* using statistical calculations.^[36] Their study showed that the oxygen functionalities tend to diffuse, agglomerate, and form highly oxidized domains on GO.

We decided to extend the most efficient strategy of double functionalization, based on the combination of epoxide opening and esterification, to another source of GO (from Grupo Antolin, named **GO-A**, see Supporting Information). This sample contains less aggregated sheets and it is much more dispersible in water compared to GO from NanoInnova. As a consequence, **GO-A** is more suitable for applications requiring high water dispersibility such as those in nanomedicine. In this case, we used two orthogonal protecting groups, namely Boc and 1-(2-nitrophenyl)ethyl carbamate,^[38-40] to protect the two primary amines grafted onto the surface of GO in order to give the possibility of further selective amine derivatization. Reducing and drastic conditions to remove protecting groups usually affect GO and this is the reason why they should be avoided. In this context, photocleavable moieties are attractive alternative protecting groups.

We first performed the epoxide opening reaction by adding compound **1** to **GO-A** giving **GO_A-OE** (Scheme 2). Afterwards, compound **5** (synthesized in two steps via intermediate **4**, Scheme S8) was added to **GO_A-OE** in the presence of EDC and DMAP as coupling agents to obtain **GO_A-OE-EST** (Scheme 2).



Scheme 2. Double functionalization of GO performed by combining the epoxide opening with esterification on **GO-A** (each reaction is shown only on one functional group for clarity reasons).

The final conjugate was first treated with HCl in 1,4-dioxane to cleave the Boc group and then irradiated at 365 nm to cleave the 1-(2-nitrophenyl)ethyl carbamate group (Scheme S9). The level of functionalization was determined by the Kaiser test giving an average amine loading of 34 $\mu\text{mol/g}$ and 71 $\mu\text{mol/g}$ after Boc deprotection and photocleavage of **GO_A-OE-EST**, respectively. (Table S2). We deduced that the level of functionalization for the esterification reaction was 37 $\mu\text{mol/g}$, which is consistent with the value obtained when the photocleavage was performed before Boc deprotection (41 $\mu\text{mol/g}$). The reactivity of **GO-A** is relatively similar to that of **GO-N** towards esterification (52 $\mu\text{mol/g}$). Nevertheless, we do not have clear explanations for the lower amine loading obtained for the epoxide opening reaction on **GO-A** compared to **GO-N**. A possible reason may be a batch-to-batch variability.

XPS confirmed the introduction of the two chains as 1.72% and 3.39% of nitrogen was found for the first and the second step, respectively (Figure 1), while only 0.46%N was obtained for the control sample **GO_A-OE_CONT** (data not shown). Moreover, in the N1s high resolution spectra it was possible to identify the characteristic peak for the nitro moiety of the 1-(2-nitrophenyl)ethyl group at 405.7 ± 0.2 eV in addition to the peak at 399-400 eV corresponding to amines and amides (Figure 1h). As previously mentioned, because of the complexity of the deconvolution of the C1s peak, no conclusion on the success of the reactions can be drawn from the C1s spectra (Figure S9).

Nevertheless, an increase in the C=O peak was detected in the O1s high resolution spectra, confirming the introduction of compounds **1** and **5** (Figure 1d,g). The first derivative of the C KLL spectra showed no significant difference in distance for the derivatized GO samples compared to **GO-A**, indicating that the double functionalization strategy preserved the π - π conjugated structure of GO (Figure S9d). This was also confirmed by the small increase of the C/O ratio (2.33 for **GO-A** vs. 2.47 for **GO_A-OE** and 2.75 **GO_A-OE-EST**, respectively).

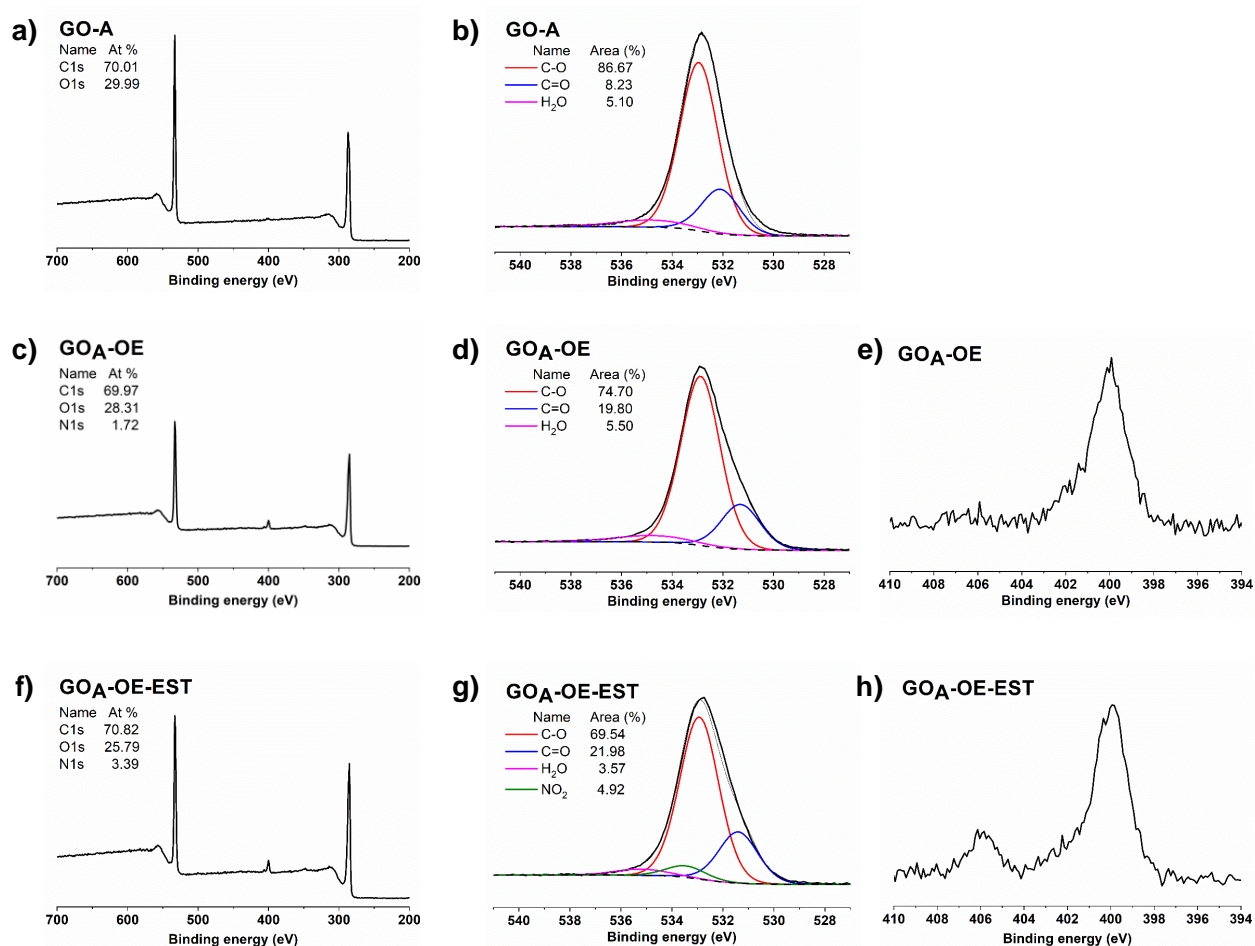


Figure 1. (a) (c) (f) XPS survey spectra of **GO-A**, **GO_A-OE**, and **GO_A-OE-EST**; (b) (d) (g) O1s of **GO-A**, **GO_A-OE**, and **GO_A-OE-EST**; (e) (h) N1s spectra of **GO_A-OE** and **GO_A-OE-EST**.

The thermogravimetric curves of **GO_A-OE** and **GO_A-OE-EST** clearly showed different thermal profiles compared with their respective controls **GO_A-OE-CONT** and **GO_A-OE-EST-CONT** (Figure 2 and Scheme S10). We observed a higher weight loss for **GO_A-OE-EST** compared to **GO_A-OE** and the control samples in the temperature range of 400-800°C, which is indicative of a higher amount of functional groups, confirming that GO was successfully doubly functionalized. The first derivatives of the TGA curves (DTG) are shown in Figure S10 and the peaks indicate the temperature of the maximum rate of change on the weight loss curves (also known as the inflection points). The DTG curves allowed comparing precisely the thermal profiles of the different samples. The first

main slope in the TGA of **GO_A-OE** occurred at lower temperature (centered at 184°C) compared with **GO-A** (220°C) and **GO_A-OE_CONT** (200°C). It can be explained by the introduction of the TEG chain covalently grafted on **GO-A**. The TGA of compound **1** shows that it was degraded at around 184°C, while the 1-(2-nitrophenyl)ethyl derivative **5** was degraded at 262°C. After esterification the main slope occurred at higher temperature (196°C), which can be attributed to the grafting of compound **5**. In addition, the weight loss between 50 and 220°C was lower after the second reaction, which can be explained by a lower amount of OH groups available on the GO surface due to the derivatization of the hydroxyls. An additional peak appeared at 370°C in the DTG of both **GO_A-OE** and **GO_A-OE-EST**, whereas it was absent in the DTG of the control samples, which could be assigned to the presence of the functional groups on GO (Figure S10). Overall, TGA confirmed that **GO-A** was successfully doubly functionalized *via* combined epoxide ring opening and esterification reactions.

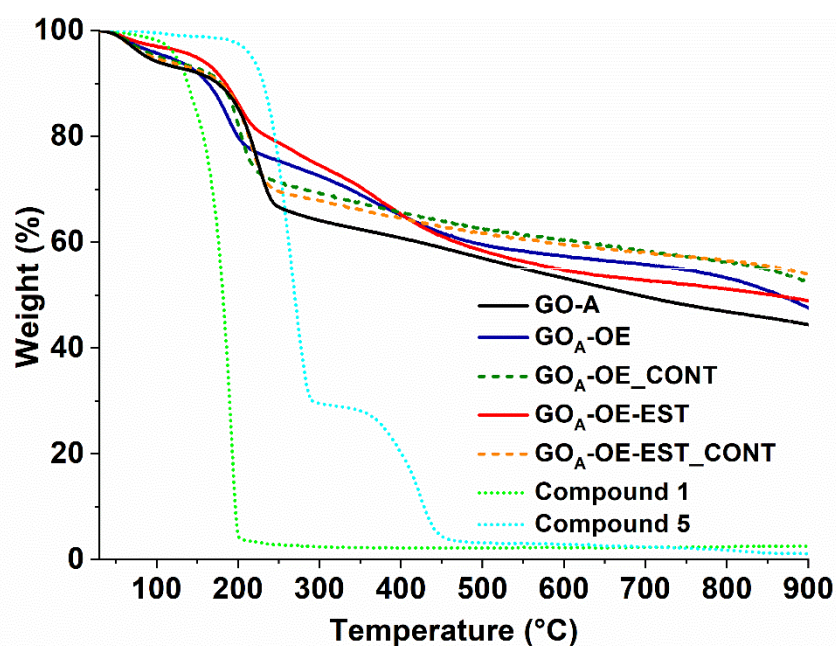


Figure 2. TGA of **GO-A**, **GO_A-OE**, **GO_A-OE-EST**, **GO_A-OE_CONT**, **GO_A-OE-EST_CONT**, and compounds **1** and **5** performed under inert atmosphere.

TEM showed that the morphology of **GO-A** was not affected by the different treatments (Figure S1e,f).

Finally, **GO_A-OE-EST** was characterized by CP and quantitative DP MAS ¹³C NMR (Figure 3). We estimated that **GO-A** is constituted of 15% epoxides, 25% hydroxyls, and 45% C=C bond (Table S3b). Compared to **GO-A**, the peak attributed to the epoxides at 60 ppm decreased in the DP spectrum because of the introduction of **1** (Figure 3, bottom spectrum), as previously observed in the case of

GO-N. At about 165 ppm we were delighted to see the peak of the ester group in both DP and CP spectra, confirming the introduction of **5**. Beside the ester peak, we could also observe the appearance of other new peaks that confirmed the introduction of both chains, in particular the peak of the carbamate of the Boc group and 1-(2-nitrophenyl)ethyl moiety at 156 ppm, the C-N bond of **1** and **5** at 39 ppm, as well as the CH₃ of **1** and CH₂ from the aliphatic chain of **5** at 26 ppm.

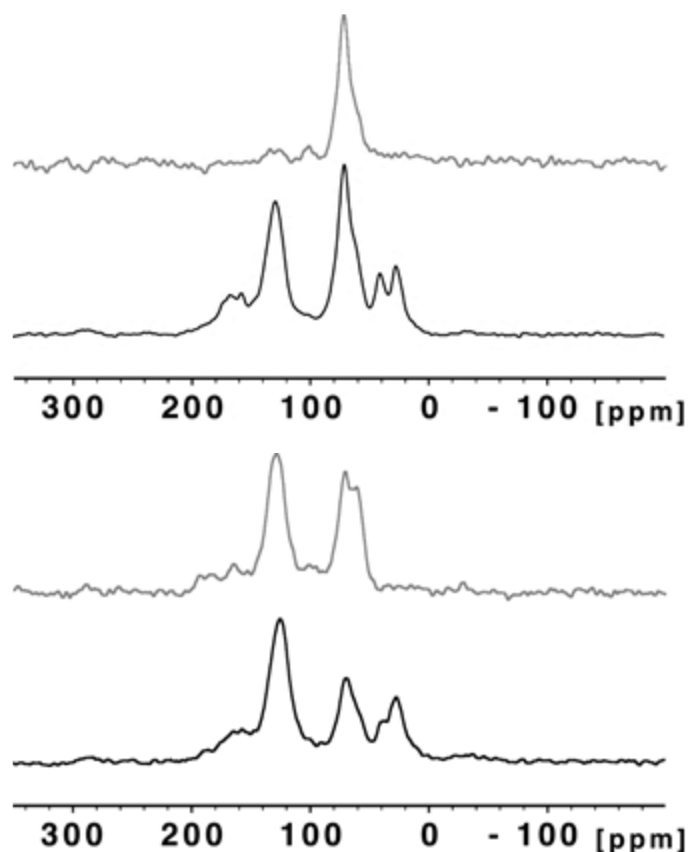


Figure 3. Qualitative CP (top) and quantitative (bottom) DP ¹³C MAS NMR spectra of **GO-A** (grey) and **GOA-OE-EST** (black).

Based on a combination of characterization techniques, we efficiently proved the introduction of both chains on **GO-A** and we also demonstrated that the strategy is successful on different sources of GO. Nevertheless, the level of functionalization of **GO-A** was lower compared to **GO-N**, pointing out that various sources of GO can have different chemical reactivity. In addition, MAS NMR showed that **GO-N** and **GO-A** do not have exact composition (Table S3). In particular, in the ¹³C CP MAS NMR spectra the peak at ~130 ppm is less intense for **GO-A** compared to **GO-N** (Figure 3 and S8, top grey spectra), whereas in the quantitative ¹³C DP MAS NMR spectra this peak is slightly more intense (45%) as in the case of **GO-N** (37%) (bottom grey spectra in Figure 3 and S8, Table S3). This result is indicative of a different distribution of protonated carbon atoms in both GO samples.^[22] The protonated carbon atoms seem to be homogeneously distributed on the surface of **GO-N**, thus the protons are able to transfer magnetization to the carbon atoms in close proximity. On the contrary,

there seem to be fewer protonated carbon atoms, probably in the form of clusters, in the case of **GO-A**. Therefore, only the protons at the cluster border are capable of transferring magnetization to the adjacent carbon atoms, which can explain the low intense peak at ~130 ppm for **GO-A** in comparison to **GO-N** in the CP spectra. This observation indicates that the localization of functional groups on GO surface is not homogeneous and can vary from one source to the other.

Conclusion

We have investigated three different strategies for the covalent double functionalization of GO through the chemoselective derivatization of the epoxides and the hydroxyl groups. The most efficient method appeared to be the combination of the opening of the epoxides and the esterification of the hydroxyls. A thorough characterization by different techniques including XPS, TGA, MAS NMR, and the Kaiser test confirmed the occurrence of the two successive reactions. The presence of amine functions allows further derivatization with molecules of interest in mild conditions such as amidation. The use of two orthogonally protected amino chains opens opportunities for the controlled derivatization of the amine functions with two different molecules *via* a selective and sequential cleavage of the orthogonal protecting groups. The multifunctionalized GO holds a high potential for future applications in different fields and in particular in nanomedicine where GO could be used as a multimodal platform for therapeutic and imaging applications.

Experimental Section

Materials and Methods are detailed in the SI, as well as the synthesis of compounds **4** and **5**, protocols for the functionalization of GO, reaction schemes, and complementary characterization by the Kaiser test, XPS, TGA, TEM, and NMR.

Acknowledgements

This work was supported by the Centre National de la Recherche Scientifique (CNRS) and by the International Center for Frontier Research in Chemistry (icFRC). The authors gratefully acknowledge financial support from EU GRAPHENE Flagship project (no. 785219), from EU MSCA-RISE projet CARBO-IMmap (no. 734381) and from the Agence Nationale de la Recherche (ANR) through the LabEx project Chemistry of Complex Systems (ANR-10-LABX-0026_CSC). S.G. is indebted to the China Scholarship Council for supporting his PhD internship. We also wish to acknowledge C. Royer and V. Demais for help with TEM analyses at the Plateforme Imagerie in Vitro at the INCI (Strasbourg, France).

References

- [1] D. Chen, H. Feng, J. Li, *Chem. Rev.* **2012**, *112*, 6027–6053.
- [2] P. Zheng, N. Wu, *Chem. Asian J.* **2017**, *12*, 2343–2353.
- [3] Z. Gu, S. Zhu, L. Yan, F. Zhao, Y. Zhao, *Adv. Mater.* **2019**, *31*, 1800662.
- [4] G. Reina, J. M. González-Domínguez, A. Criado, E. Vázquez, A. Bianco, M. Prato, *Chem. Soc. Rev.* **2017**, *46*, 4400–4416.
- [5] D.-K. Ji, C. Ménard-Moyon, A. Bianco, *Adv. Drug Deliv. Rev.* **2019**, *138*, 211–232.
- [6] G. Seber, J. Muñoz, S. Sandoval, C. Rovira, G. Tobias, M. Mas-Torrent, N. Crivillers, *Adv. Mater. Interfaces* **2018**, *5*, 1701072.
- [7] B. Cai, S. Wang, L. Huang, Y. Ning, Z. Zhang, G.-J. Zhang, *ACS Nano* **2014**, *8*, 2632–2638.
- [8] D. R. Dreyer, S. Park, C. W. Bielawski, R. S. Ruoff, *Chem. Soc. Rev.* **2010**, *39*, 228–240.
- [9] D. R. Dreyer, A. D. Todd, C. W. Bielawski, *Chem. Soc. Rev.* **2014**, *43*, 5288–5301.
- [10] S. Eigler, A. Hirsch, *Angew. Chem. Int. Ed.* **2014**, *53*, 7720–7738.
- [11] V. Georgakilas, M. Otyepka, A. B. Bourlinos, V. Chandra, N. Kim, K. C. Kemp, P. Hobza, R. Zboril, K. S. Kim, *Chem. Rev.* **2012**, *112*, 6156–6214.
- [12] I. A. Vacchi, C. Spinato, J. Raya, A. Bianco, C. Ménard-Moyon, *Nanoscale* **2016**, *8*, 13714–13721.
- [13] R. Imani, S. Prakash, H. Vali, S. Faghihi, *Biomater. Sci.* **2018**, *6*, 1636–1650.
- [14] A. Rezaei, O. Akhavan, E. Hashemi, M. Shamsara, *Chem. Mater.* **2016**, *28*, 3004–3016.
- [15] S. Luo, Z. Yang, X. Tan, Y. Wang, Y. Zeng, Y. Wang, C. Li, R. Li, C. Shi, *ACS Appl. Mater. Interfaces* **2016**, *8*, 17176–17186.
- [16] K.-C. Mei, N. Rubio, P. M. Costa, H. Kafa, V. Abbate, F. Festy, S. S. Bansal, R. C. Hider, K. T. Al-Jamal, *Chem. Commun.* **2015**, *51*, 14981–14984.
- [17] S. Guo, Y. Nishina, A. Bianco, C. Ménard-Moyon, *Angew. Chem. Int. Ed.*, DOI: 10.1002/anie.201913461.
- [18] P. Pérez-Martínez, J. M. Galvan-Miyoshi, J. Ortiz-López, *J. Mater. Sci.* **2016**, *51*, 10782–10792.
- [19] S. Pei, H.-M. Cheng, *Carbon* **2012**, *50*, 3210–3228.
- [20] M. Rogala, P. Dabrowski, P. J. Kowalczyk, I. Wlasny, W. Kozłowski, A. Busiakiewicz, I. Karaduman, L. Lipinska, J. M. Baranowski, Z. Klusek, *Carbon* **2016**, *103*, 235–241.
- [21] A. M. Dimiev, L. B. Alemany, J. M. Tour, *ACS Nano* **2013**, *7*, 576–588.
- [22] I. A. Vacchi, J. Raya, A. Bianco, C. Ménard-Moyon, *2D Mater.* **2018**, *5*, 035037.
- [23] S. Eigler, C. Dotzer, A. Hirsch, M. Enzelberger, P. Müller, *Chem. Mater.* **2012**, *24*, 1276–1282.
- [24] S. Stankovich, D. A. Dikin, R. D. Piner, K. A. Kohlhaas, A. Kleinhammes, Y. Jia, Y. Wu, S. T. Nguyen, R. S. Ruoff, *Carbon* **2007**, *45*, 1558–1565.

- [25] J. I. Paredes, S. Villar-Rodil, A. Martínez-Alonso, J. M. D. Tascón, *Langmuir* **2008**, *24*, 10560–10564.
- [26] S. Kim, S. Zhou, Y. Hu, M. Acik, Y. J. Chabal, C. Berger, W. de Heer, A. Bongiorno, E. Riedo, *Nature Mater.* **2012**, *11*, 544–549.
- [27] C. K. Chua, M. Pumera, *Small* **2015**, *11*, 1266–1272.
- [28] P. V. Kumar, N. M. Bardhan, S. Tongay, J. Wu, A. M. Belcher, J. C. Grossman, *Nature Chem.* **2014**, *6*, 151–158.
- [29] Z. Lin, Y. Yao, Z. Li, Y. Liu, Z. Li, C.-P. Wong, *J. Phys. Chem. C* **2010**, *114*, 14819–14825.
- [30] J. T. Paci, T. Belytschko, G. C. Schatz, *J. Phys. Chem. C* **2007**, *111*, 18099–18111.
- [31] M. C. Biesinger. X-ray Photoelectron Spectroscopy (XPS) Reference Pages. Available from: <http://www.xpsfitting.com/>
- [32] J. C. Lascovich, R. Giorgi, S. Scaglione, *Appl. Surf. Sci.* **1991**, *47*, 17–21.
- [33] A. J. Barlow, S. Popescu, K. Artyushkova, O. Scott, N. Sano, J. Hedley, P. J. Cumpson, *Carbon* **2016**, *107*, 190–197.
- [34] A. Hunt, D. A. Dikin, E. Z. Kurmaev, T. D. Boyko, P. Bazylewski, G. S. Chang, A. Moewes, *Adv. Funct. Mater.* **2012**, *22*, 3950–3957.
- [35] H. Pieper, C. E. Halbig, L. Kovbasyuk, M. R. Filipovic, S. Eigler, A. Mokhir, *Chem. Eur. J.* **2016**, *22*, 15389–15395.
- [36] S. Zhou, A. Bongiorno, *Sci. Rep.* **2013**, *3*, 2484.
- [37] K. Erickson, R. Erni, Z. Lee, N. Alem, W. Gannett, A. Zettl, *Adv. Mater.* **2010**, *22*, 4467–4472.
- [38] C. G. Bochet, *J. Chem. Soc., Perkin Trans. 1* **2002**, 125–142.
- [39] M. Kessler, R. Glatthar, B. Giese, C. G. Bochet, *Org. Lett.* **2003**, *5*, 1179–1181.
- [40] R. S. Givens, P. G. Conrad, A. L. Yousef, J.-III Lee, Photoremovable Protecting Groups, 2003. p. 2904. In: CRC Handbook of Organic Photochemistry and Photobiology (Eds.: W. M. Horspool, F. Lenci).